SCIENTIFIC REPORTS

OPEN

In vivo synaptic activity-independent co-uptakes of amyloid β_{1-42} and Zn^{2+} into dentate granule cells in the normal brain

Received: 25 October 2018
Accepted: 10 April 2019
Published online: 24 April 2019

Haruna Tamano[1], Naoya Oneta[1], Aoi Shioya[1], Paul A. Adlard[2], Ashley I. Bush[2] & Atsushi Takeda[1]

Neuronal amyloid β_{1-42} ($A\beta_{1-42}$) accumulation is considered an upstream event in Alzheimer's disease pathogenesis. Here we report the mechanism on synaptic activity-independent $A\beta_{1-42}$ uptake *in vivo*. When $A\beta_{1-42}$ uptake was compared in hippocampal slices after incubating with $A\beta_{1-42}$, *In vitro* $A\beta_{1-42}$ uptake was preferentially high in the dentate granule cell layer in the hippocampus. Because the rapid uptake of $A\beta_{1-42}$ with extracellular Zn^{2+} is essential for $A\beta_{1-42}$-induced cognitive decline *in vivo*, the uptake mechanism was tested in dentate granule cells in association with synaptic activity. *In vivo* rapid uptake of $A\beta_{1-42}$ was not modified in the dentate granule cell layer after co-injection of $A\beta_{1-42}$ and tetrodotoxin, a Na^+ channel blocker, into the dentate gyrus. Both the rapid uptake of $A\beta_{1-42}$ and Zn^{2+} into the dentate granule cell layer was not modified after co-injection of CNQX, an AMPA receptor antagonist, which blocks extracellular Zn^{2+} influx, Both the rapid uptake of $A\beta_{1-42}$ and Zn^{2+} into the dentate granule cell layer was not also modified after either co-injection of chlorpromazine or genistein, an endocytic repressor. The present study suggests that $A\beta_{1-42}$ and Zn^{2+} are synaptic activity-independently co-taken up into dentate granule cells in the normal brain and the co-uptake is preferential in dentate granule cells in the hippocampus. We propose a hypothesis that Zn-$A\beta_{1-42}$ oligomers formed in the extracellular compartment are directly incorporated into neuronal plasma membranes and form Zn^{2+}-permeable ion channels.

Alzheimer's disease (AD) has a preclinical phase of 20–30 years prior to clinical onset and is the most common cause of dementia[1,2]. Amyloid-β (Aβ) peptides are produced by processing of amyloid precursor protein (APP)[3,4] and have a characteristic of self-assembly into oligomers in the extracellular compartment[5]. $A\beta_{1-40}$ and $A\beta_{1-42}$ are the two major isoforms[6]. $A\beta_{1-42}$ more readily forms oligomers than $A\beta_{1-40}$ and is more neurotoxic[7]. Formation and propagation of misfolded aggregates of $A\beta_{1-42}$ may contribute to AD pathogenesis rather than those of $A\beta_{1-40}$. C-Terminal carboxylate anion of $A\beta_{1-42}$, which forms the C-terminal hydrophobic core, leads to accelerate neurotoxic oligomerization[8]. C-Terminal Ala42 that is absent in $A\beta_{1-40}$ forms a salt bridge with Lys28 and constructs a self-recognition molecular switch. The switch is the $A\beta_{1-42}$-mediated self-replicating amyloid-propagation machinery[9].

In AD pathogenesis, Zn^{2+} has been implicated by inducing rapid Aβ oligomerization[10–12]. The aggregation property of $A\beta_{1-42}$ is accelerated with Zn^{2+}, followed by much higher affinity of $A\beta_{1-42}$ (K_d = ~3–30 nM) to Zn^{2+} than $A\beta_{1-40}$ (K_d = 0.1–60 μM), which leads to neuronal Zn-$A\beta_{1-42}$ uptake and then synaptic dysfunction. In the hippocampus, $A\beta_{1-42}$ released into the extracellular compartment can capture Zn^{2+}, which is estimated to be approximately 10 nM in the extracellular fluid[13], even at 500 pM $A\beta_{1-42}$ *in vivo*. We have reported that $A\beta_{1-42}$ takes Zn^{2+} as a cargo into dentate granule cells in the normal brain, followed by cognitive decline[14–16]. Although the mechanism of Zn-$A\beta_{1-42}$ uptake remains to be solved, extracellular Zn^{2+} is essential for $A\beta_{1-42}$ uptake into dentate granule cells[15].

[1]Department of Neurophysiology, School of Pharmaceutical Sciences, University of Shizuoka, 52-1 Yada, Suruga-ku, Shizuoka, 422-8526, Japan. [2]The Florey Institute of Neuroscience and Mental Health, The University of Melbourne, Parkville, VIC, 3052, Australia. Correspondence and requests for materials should be addressed to A.T. (email: takedaa@u-shizuoka-ken.ac.jp)

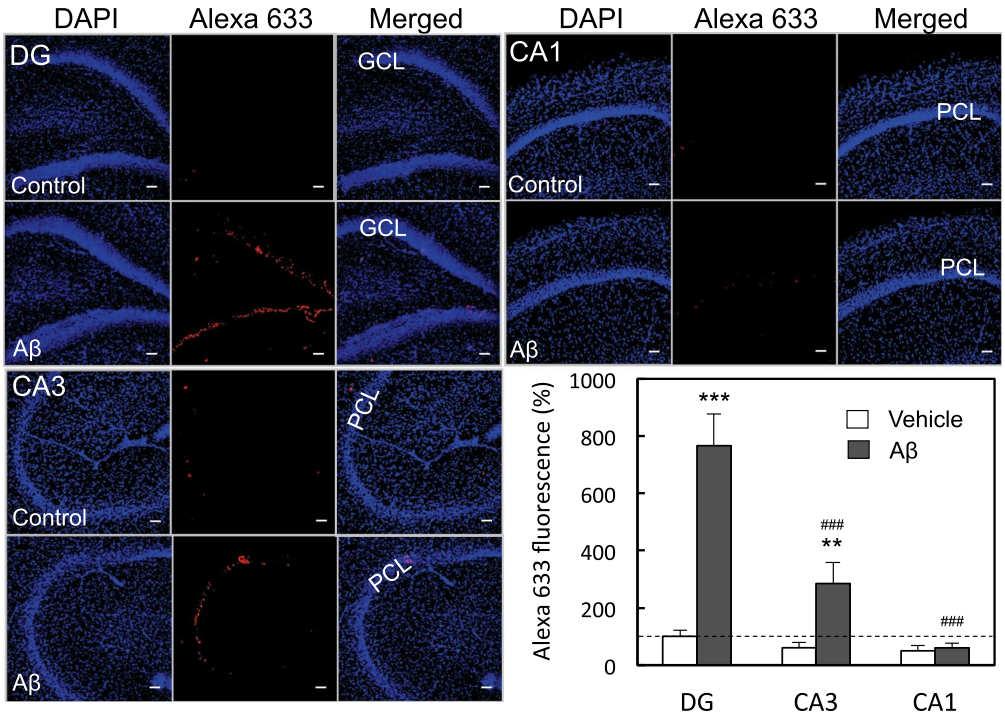

Figure 1. *In vitro* $A\beta_{1-42}$ uptake in the hippocampus. Aβ immunostaining was determined in the dentate gyrus (DG), the CA3, and the CA1 15 min after incubation with 50 μM $A\beta_{1-42}$ in ACSF. GCL, dentate granule cell layer; PCL, pyramidal cell layer. Aβ uptake in the GCL (n = 32), CA3 PCL (n = 22), and CA1 PCL (n = 22) was determined with Alexa 633 intensity, which was represented by the ratio to Alexa 633 intensity in the control GCL without 50 μM $A\beta_{1-42}$ in ACSF expressed as 100% (lower-right). Alexa 633 intensity in the control CA3 PCL and the control CA1 PCL was also represented by the ratio to Alexa 633 intensity in the control GCL. $^{**}p < 0.01$, $^{***}p < 0.001$, vs. each control with vehicle (DG, n = 29; CA3, n = 20; CA1, n = 20), $^{\#\#\#}p < 0.001$, vs. DG with $A\beta_{1-42}$. Bar, 50 μm.

It had been reported that Aβ oligomers form Ca^{2+}-permeable plasma membrane pores that form Aβ channels, leading to a disruption of neuronal Ca^{2+} homeostasis[17,18], which may be linked with synaptic dysfunction and neurodegeneration[19]. Aβ-mediated Ca^{2+} channels interact with Zn^{2+} and Zn^{2+} blocks extracellular Ca^{2+} influx in the range of high micromolar concentrations (>250 μM)[20], although the gating kinetics and Ca^{2+} permeability of Aβ pores are not well understood[21].

In the present study, we postulate that Zn-$A\beta_{1-42}$ oligomers formed in the extracellular compartment form Zn^{2+}-permeable plasma membrane pores, based on the evidence of permeation of Zn^{2+} through Ca^{2+} channels[22,23]. Here we report the mechanism on synaptic activity-independent $A\beta_{1-42}$ uptake *in vivo*.

Results

When $A\beta_{1-42}$ is bound to extracellular Zn^{2+} *in vivo*, $A\beta_{1-42}$ is rapidly taken up into dentate granule cells and affects memory via attenuated LTP[14–16]. Both uptake of $A\beta_{1-42}$ and Zn^{2+} are observed 5 min after $A\beta_{1-42}$ injection into the dentate gyrus, followed by Aβ toxicity and are blocked by coinjection of CaEDTA, an extracellular Zn^{2+} chelator, followed by blockade of Aβ toxicity. Thus, we need to clarify the mechanism of the rapid uptake of $A\beta_{1-42}$ *in vivo*, which is linked with Aβ toxicity. On the other hand, endogenous Zn^{2+} released from the hippocampal slices promotes $A\beta_{1-42}$ uptake (retention), which is determined by *in vitro* Aβ immunohistochemistry (monoclonal antibody 4G8), in the absence of additional extracellular Zn^{2+} [15].

In the present study, $A\beta_{1-42}$ uptake was determined in rat hippocampal slices 15 min after incubation with $A\beta_{1-42}$, $A\beta_{1-42}$ uptake was preferentially high in the dentate granule cell layer in the hippocampus, compared with the CA3 and CA1 pyramidal cell layer (Fig. 1).

To examine the involvement of neuronal activity in $A\beta_{1-42}$ uptake, $A\beta_{1-42}$ and tetrodotoxin, a Na^+ channel blocker, was co-injected into the dentate gyrus of rats. The present dose (15 μM) of tetrodotoxin was determined based on the *in vivo* action as a Na^+ channel blocker (10 μM)[24]. $A\beta_{1-42}$ uptake was determined by *ex vivo* Aβ immunohistochemistry 5 min after the co-injection. The rapid uptake of $A\beta_{1-42}$ was not modified in the dentate granule cell layer even by co-injection of tetrodotoxin (Fig. 2).

AMPA receptor activation induces extracellular Zn^{2+} influx *in vivo*, which is blocked in the presence of 2 mM CNQX, and the excess influx leads to cognitive decline via attenuated LTP[25,26]. The present dose of CNQX (2 mM) was used according to the previous papers. Both the rapid uptake of $A\beta_{1-42}$ and Zn^{2+} into the dentate granule cell layer was not modified by co-injection of CNQX (Fig. 3), suggesting $A\beta_{1-42}$-mediated extracellular Zn^{2+} influx.

We examined whether endocytosis is involved in the rapid uptake of $A\beta_{1-42}$ and Zn^{2+}. Chlorpromazine (500 μM), a clathrin/caveolae-mediated endocytosis blocker, was used based on the *in vivo* action as a blocker

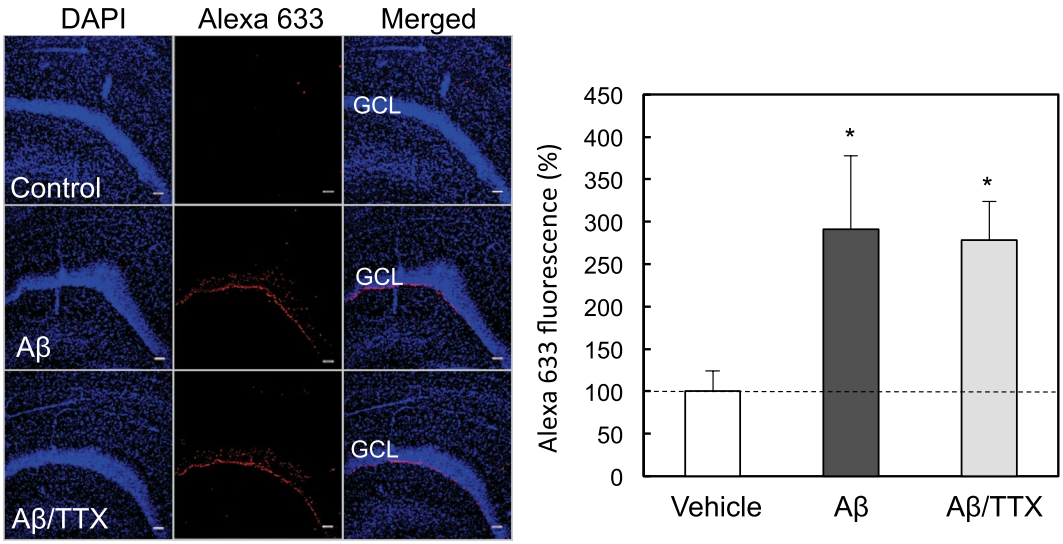

Figure 2. *In vivo* uptake of $A\beta_{1-42}$ in the dentate gyrus in the presence of tetrodotoxin. $A\beta_{1-42}$ immunostaining was determined in the dentate gyrus 5 min after injection of 50 μM $A\beta_{1-42}$ (n = 6), and 50 μM $A\beta_{1-42}$ + 15 μM tetrodotoxin (n = 8) in ACSF into the dentate gyrus of anesthetized rats (left). GCL, dentate granule cell layer. Bar, 50 μm. $A\beta_{1-42}$ uptake in the dentate granule cell layer determined with Alexa 633 intensity, which is represented by the ratio to the control (n = 12) without 50 μM $A\beta_{1-42}$ in ACSF expressed as 100%. *$p < 0.05$, vs. control.

(200 μM)[27]. Genistein (250 μM), a caveolae/raft-mediated endocytosis blocker, was used based on the blocking effect on the primary entry pathway for aquareovirus (<200 μM)[28]. Both the rapid uptake of $A\beta_{1-42}$ and Zn^{2+} into the dentate granule cell layer was not also modified by either co-injection of chlorpromazine (Fig. 4) or genistein (Fig. 5).

Discussion

In vivo LTP at medial perforant pathway-dentate granule cell synapses, which is closely linked to object recognition memory[29], is not affected even under perfusion with 1,000 nM $A\beta_{1-42}$ in ACSF without Zn^{2+}, but attenuated under pre-perfusion with 500 pM $A\beta_{1-42}$ in ACSF containing 10 nM Zn^{2+}. The attenuation is rescued by extracellular Zn^{2+}-chelation with CaEDTA. These data indicate that high picomolar $A\beta_{1-42}$ captures extracellular Zn^{2+} and subsequently attenuates LTP[15]. The evidence is consistent with $A\beta_{1-42}$-induced object recognition memory deficit, which is also rescued by CaEDTA and ZnAF-2DA, an intracellular Zn^{2+} chelator[13]. Thus, extracellular Zn^{2+} is essential for $A\beta_{1-42}$-induced cognitive decline via attenuated LTP in the normal brain, consistent with *in vivo* complete blocking rapid uptake of $A\beta_{1-42}$ and Zn^{2+} into dentate granule cells after co-injection of $A\beta_{1-42}$ and CaEDTA into the dentate gyrus[15]. In the present study, we tested the uptake mechanism of $A\beta_{1-42}$ oligomers *in vitro* and *in vivo*.

When $A\beta_{1-42}$ uptake was determined in hippocampal slices after incubation with $A\beta_{1-42}$, $A\beta_{1-42}$ uptake was preferentially high in the dentate granule cell layer in the hippocampus. $A\beta_{1-42}$ uptake was also considerably high in the CA3 pyramidal cell layer, while $A\beta_{1-42}$ uptake was not observed in the CA1 pyramidal cell layer. Extracellular Zn^{2+} interaction with $A\beta_{1-42}$ is essential for $A\beta_{1-42}$ uptake into dentate granule cells *in vivo* and its essentiality is the same even under *in vitro* hippocampal slice condition[15]. Endogenous Zn^{2+} release from the hippocampal slices is required for the $A\beta_{1-42}$ uptake. In hippocampal slices bathed in ACSF without Zn^{2+}, extracellular Zn^{2+} level determined with ZnAF-2 is the highest in the hilus close to the dentate granule cell layer and the second highest in the stratum lucidum close to the CA3 pyramidal cell layer[30]. Endogenous Zn^{2+}, which is released from mossy fibers, may be closely linked with the $A\beta_{1-42}$ uptake. Although the Schaffer collaterals also release Zn^{2+}, it is estimated that its release is not enough for the $A\beta_{1-42}$ uptake into CA1 pyramidal cells *in vitro*. In contrast, it is estimated that $A\beta_{1-42}$ captures extracellular Zn^{2+} and is taken up into CA1 pyramidal cell *in vivo*. *In vivo* CA1 LTP is impaired after intracerebroventricular injections of Aβ peptide fragments[31], implying that extracellular Zn^{2+} is potentially involved in the impairment. Intracellular infusion of oligomerised $A\beta_{1-42}$ via passive diffusion from the patch pipette induces the rapid synaptic insertion of Ca^{2+}-permeable AMPA receptors in CA1 pyramidal cells[32]. When oligomeric $A\beta_{1-42}$ captures extracellular Zn^{2+} *in vivo*, it is also possible that intracellular oligomeric $A\beta_{1-42}$ affect neuronal functions. Postmortem studies suggest that the hippocampus and entorhinal cortex are the first brain regions to be affected in Alzheimer's disease[1,33,34]. The perforant pathway-dentate granule cell synapses are vulnerable to Aβ synapse toxicity[35], which may be linked with extracellular Zn^{2+}-mediated $A\beta_{1-42}$ uptake into dentate granule cells. This uptake may be associated with the high level of extracellular Zn^{2+} in the hilus that may be due to Zn^{2+} release form mossy fibers.

The mechanism of $A\beta_{1-42}$ uptake was tested in the dentate granule cell layer *in vivo*. When $A\beta_{1-42}$ was co-injected with tetrodotoxin, a Na^{+} channel blocker, into the dentate gyrus, the rapid uptake of $A\beta_{1-42}$ was not modified in the dentate granule cell layer. AMPA receptor activation induces extracellular Zn^{2+} influx and the

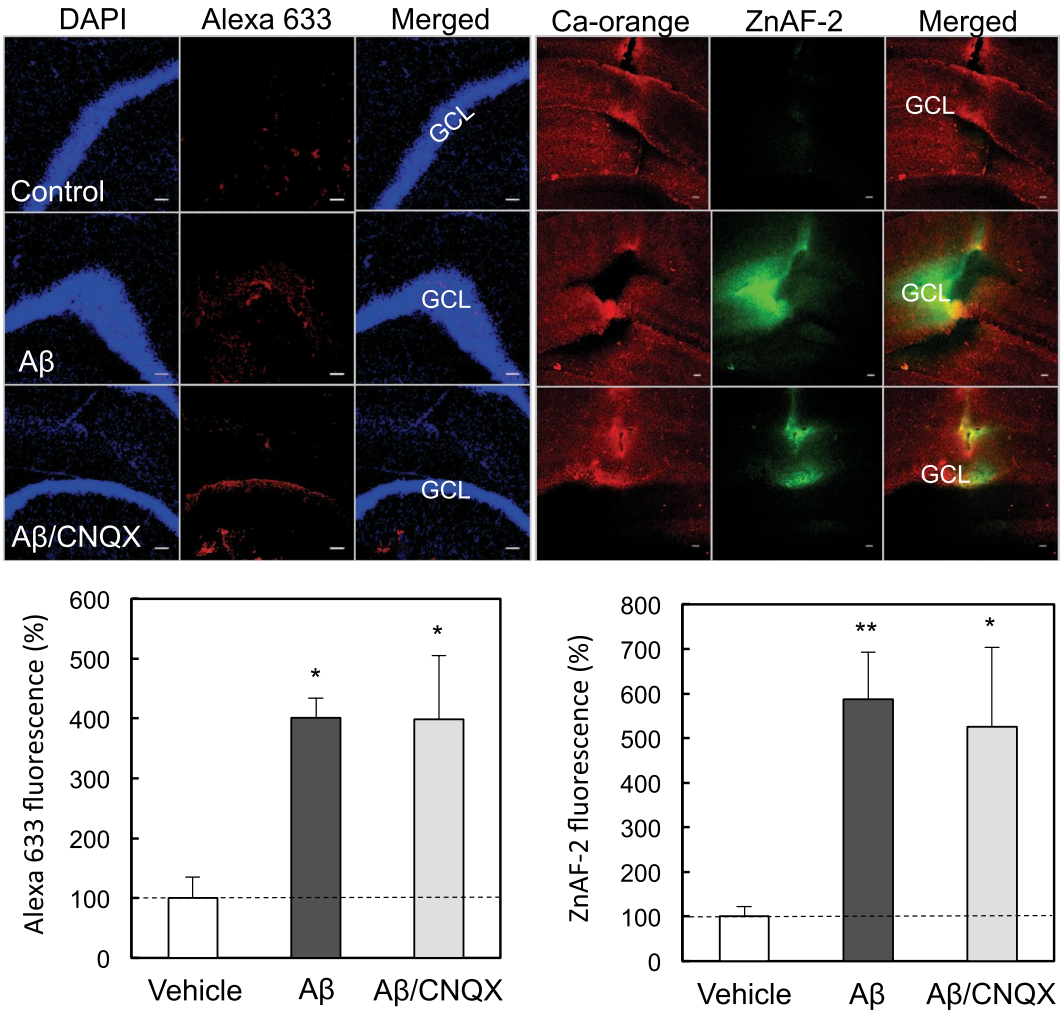

Figure 3. *In vivo* uptake of $A\beta_{1-42}$ and Zn^{2+} in the dentate gyrus in the presence of CNQX. $A\beta_{1-42}$ immunostaining (upper-left) and Zn^{2+} imaging (upper-right) were determined in the dentate gyrus 5 min after injection of 50 μM $A\beta_{1-42}$, and 50 μM $A\beta_{1-42}$ + 2 mM CNQX in ACSF into the dentate gyrus of anesthetized rats. GCL, dentate granule cell layer. Bar, 50 μm. $A\beta_{1-42}$ uptake in the dentate granule cell layer determined with Alexa 633 intensity, which is represented by the ratio to the control (control, n = 6; Aβ, n = 5; Aβ/CNQX, n = 6) without 50 μM $A\beta_{1-42}$ in ACSF expressed as 100% (lower-left). Zn^{2+} uptake in the dentate granule cell layer determined with ZnAF-2 intensity, which is represented by the ratio to the control (control, n = 11; Aβ, n = 10; Aβ/CNQX, n = 6) without 50 μM $A\beta_{1-42}$ in ACSF expressed as 100% (lower-right). *$p < 0.05$, **$p < 0.01$, vs. control.

excess influx leads to cognitive decline via attenuated LTP[25,26]. In contrast, both the rapid uptake of $A\beta_{1-42}$ and Zn^{2+} into the dentate granule cell layer was not modified after co-injection of CNQX, an AMPA receptor antagonist, suggesting that Zn-$A\beta_{1-42}$ oligomers are ionotropic glutamate receptor activation-independently taken up into dentate granule cells. Both the rapid uptake of $A\beta_{1-42}$ and Zn^{2+} into the dentate granule cell layer was not also modified after either co-injection of chlorpromazine or genistein, an endocytic repressor. It is likely that Zn-$A\beta_{1-42}$ oligomers are rapidly taken up into dentate granule cells without interaction with plasma membrane receptor proteins.

In human SH-SY5Y neuroblastoma, monomeric $A\beta_{1-42}$ is selectively internalized via clathrin- and dynamin-independent endocytosis compared to monomeric $A\beta_{1-40}$[36]. Genistein, a major phytoestrogen in soybean, may reduce the $A\beta_{1-42}$-induced cell toxicity by suppressing the formation of toxic, cell membrane penetrating $A\beta_{1-42}$ oligomers in human SH-SY5Y neuroblastoma[37]. Zn^{2+} interaction with $A\beta_{1-42}$ has not been taken into account in these *in vitro* cell culture systems, suggesting that Zn-$A\beta_{1-42}$ oligomers formed *in vivo* are taken up into dentate granule cells via a novel mechanism and causes cytotoxicity. On the other hand, Aβ production occurs in acidic vesicular organelles and contributes both to Aβ secretion and to the direct accumulation of Aβ within neurons[37]. Intracellular Aβ produced by the direct accumulation can exist as a monomeric form that further aggregates into oligomers and it may mediate pathological events[38], although it is unknown whether Zn^{2+} is involved in the pathological effects.

The Aβ ion channel hypothesis has been reported in AD pathogenesis. These authors have reported that Aβ peptides disrupt Ca^{2+} homeostasis in neurons and increase intracellular Ca^{2+} level, resulting in synaptic

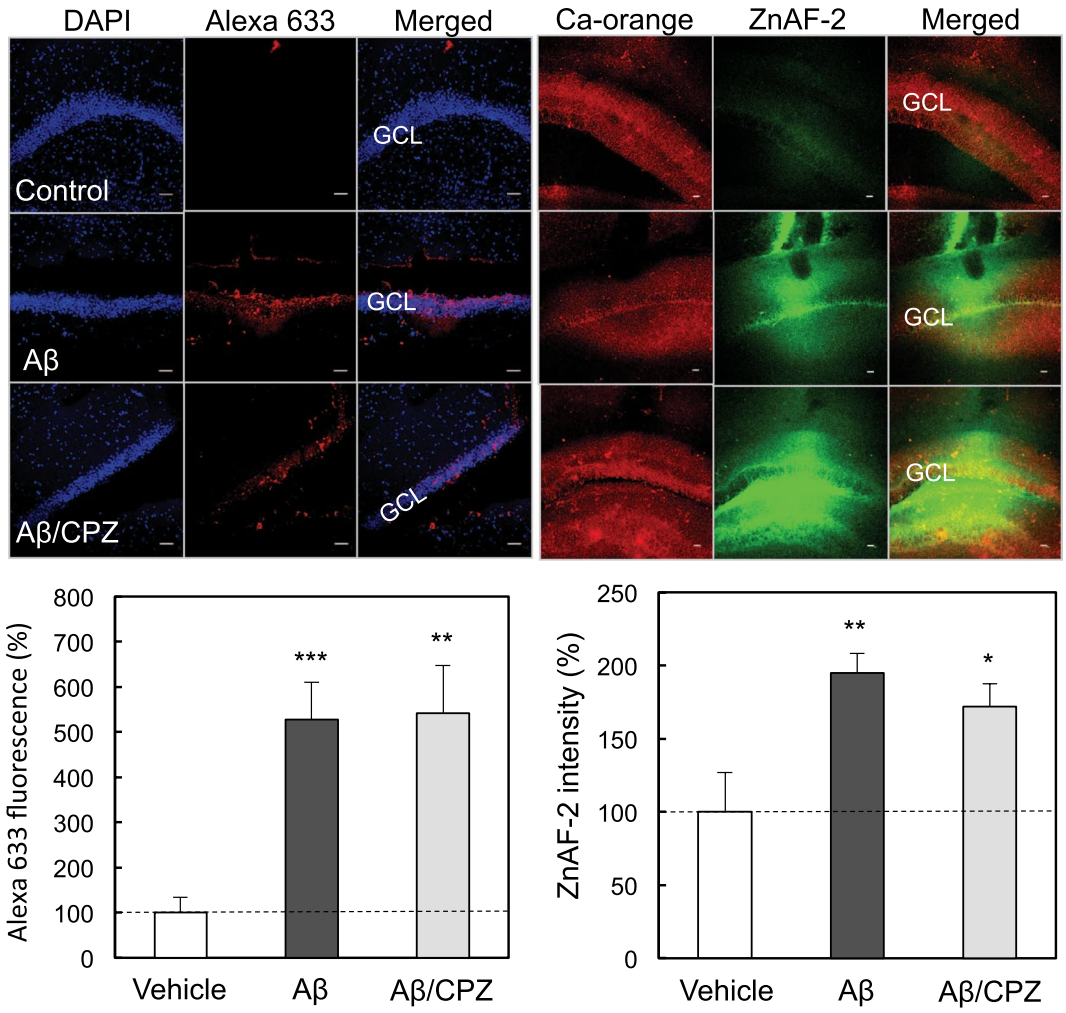

Figure 4. *In vivo* uptake of $A\beta_{1-42}$ and Zn^{2+} in the dentate gyrus in the presence of chlorpromazine (CPZ). $A\beta_{1-42}$ immunostaining (upper-left) and Zn^{2+} imaging (upper-right) were determined in the dentate gyrus 5 min after injection of 50 μM $A\beta_{1-42}$, and 50 μM $A\beta_{1-42}$ + 500 μM chlorpromazine in ACSF into the dentate gyrus of anesthetized rats. GCL, dentate granule cell layer. Bar, 50 μm. $A\beta_{1-42}$ uptake in the dentate granule cell layer determined with Alexa 633 intensity, which is represented by the ratio to the control (control, n = 11; Aβ, n = 10; Aβ/CPZ, n = 5) without 50 μM $A\beta_{1-42}$ in ACSF expressed as 100% (lower-left). Zn^{2+} uptake in the dentate granule cell layer determined with ZnAF-2 intensity, which is represented by the ratio to the control (control, n = 10; Aβ, n = 9; Aβ/CNQX, n = 11) without 50 μM $A\beta_{1-42}$ in ACSF expressed as 100% (lower-right). *p < 0.05, **p < 0.01, ***p < 0.001, vs. control.

dysfunction and neurodegeneration. The hypothesis is based on the results from *in vitro* experimental systems such as artificial membranes and neuronal culture[18,39]. Judging from capturing extracellular Zn^{2+} with high picomolar (100–500 pM) $A\beta_{1-42}$ in the hippocampal extracellular compartment, which disrupts Zn^{2+} homeostasis in neurons and increases intracellular Zn^{2+} level[14], the Aβ-mediated Ca^{2+} channel hypothesis might be changed into the $A\beta_{1-42}$-mediated Zn^{2+} channel hypothesis in AD pathogenesis. Because Aβ stain is observed around the nuclei in dentate granule cells[15], a portion of $A\beta_{1-42}$ is co-taken up with Zn^{2+} into dentate granule cells even if $A\beta_{1-42}$-mediated Zn^{2+} channels (pores) is formed in the plasma membrane.

In conclusion, the present study suggests that amyloid β_{1-42} and Zn^{2+} are synaptic activity-independently co-taken up into dentate granule cells in the normal brain and the co-uptake is preferential in dentate granule cells. We propose a hypothesis that Zn-Aβ oligomers formed in the extracellular compartment are directly incorporated into neuronal membranes and form Zn^{2+}-permeable ion channels. Because extracellular Zn^{2+} is age-relatedly increased in the rat hippocampus[40], Zn-$A\beta_{1-42}$ oligomers are more readily produced in the extracellular compartment of the aged hippocampus, followed by vulnerability to Zn-$A\beta_{1-42}$ oligomers in aging[16,41]. Therefore, controlling intracellular Zn^{2+} dysregulation may be an effective strategy for overcoming AD pathogenesis.

Experimental Procedures

Animals and chemicals. Wistar rats (male, 7–9 weeks of age) were obtained from Japan SLC (Hamamatsu, Japan). Rats were housed under the standard laboratory conditions (23 ± 1 °C, 55 ± 5% humidity) and had access

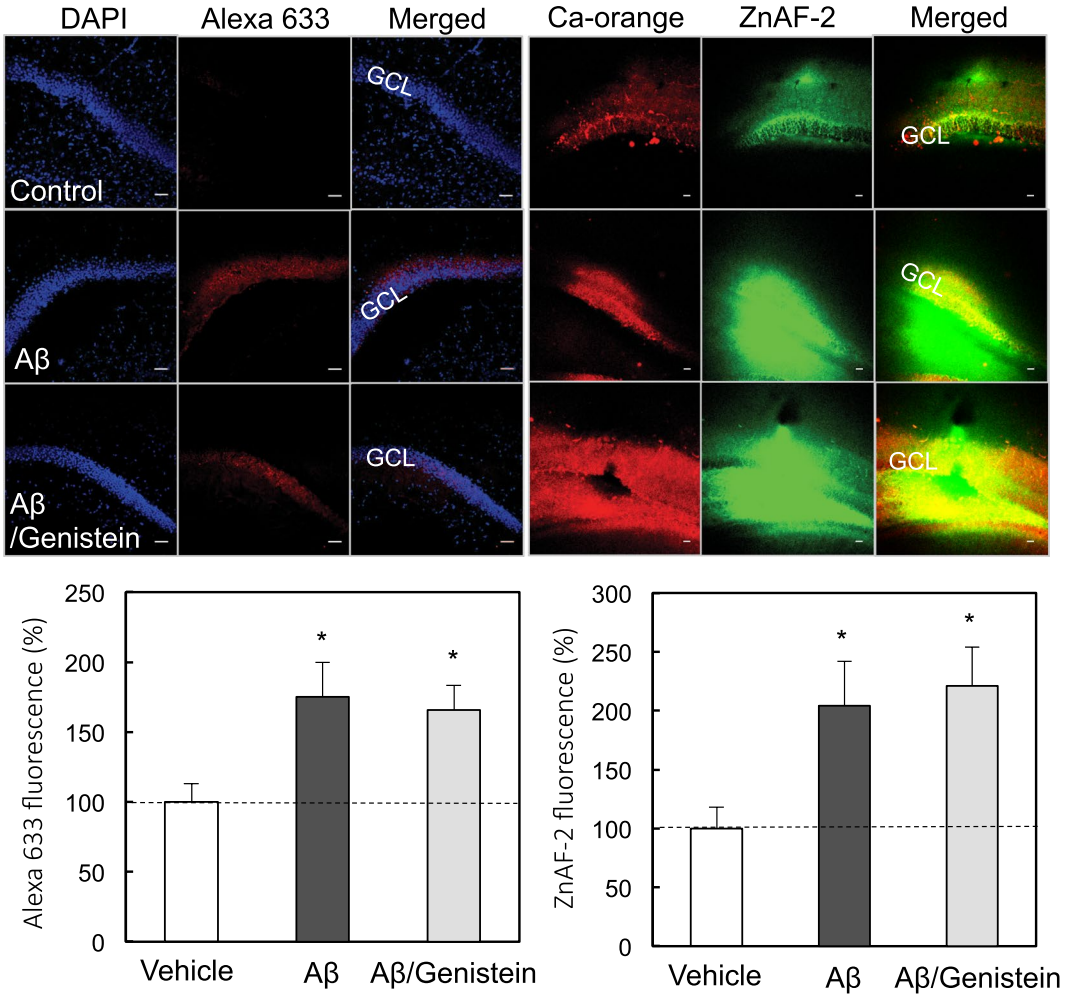

Figure 5. *In vivo* uptake of $A\beta_{1-42}$ and Zn^{2+} in the dentate gyrus in the presence of genistein. $A\beta_{1-42}$ immunostaining (upper-left) and Zn^{2+} imaging (upper-right) were determined in the dentate gyrus 5 min after injection of 50 μM $A\beta_{1-42}$, and 50 μM $A\beta_{1-42}$ + 250 μM genistein in ACSF into the dentate gyrus of anesthetized rats. GCL, dentate granule cell layer. Bar, 50 μm. $A\beta_{1-42}$ uptake in the dentate granule cell layer determined with Alexa 633 intensity, which is represented by the ratio to the control (control, n = 5; Aβ, n = 4; Aβ/genistein, n = 6) without 50 μM $A\beta_{1-42}$ in ACSF expressed as 100% (lower-left). Zn^{2+} uptake in the dentate granule cell layer determined with ZnAF-2 intensity, which is represented by the ratio to the control (control, n = 8; Aβ, n = 5; Aβ/genistein, n = 5) without 50 μM $A\beta_{1-42}$ in ACSF expressed as 100% (lower-right). *$p < 0.05$, vs. control.

to water and food *ad libitum*. Rats were used for experiments approximately 1 week after housing. All the experiments were performed according to the Guidelines for the Care and Use of Laboratory Animals in the University of Shizuoka, which refer to the American Association for Laboratory Animals Science and the guidelines laid down by the NIH (NIH Guide for the Care and Use of Laboratory Animals) in the USA. The present study has been approved by the Ethics Committee for Experimental Animals in the University of Shizuoka.

Synthetic human $A\beta_{1-42}$ was purchased from ChinaPeptides (Shanghai, China). Aβ was dissolved in saline at the time of need. $A\beta_{1-42}$ prepared in saline was mainly monomers with a small fraction of low order oligomers in SDS-PAGE[14]. ZnAF-2DA ($K_d = 2.7 \times 10^{-9}$ M for Zn^{2+}) is a membrane-permeable Zn^{2+} indicator and was kindly supplied from Sekisui Medical Co., LTD (Hachimantai, Japan). This indicator is taken up into the cells through the plasma membrane and is hydrolyzed by esterase in the cytosol to produce ZnAF-2, which does not permeate the plasma membrane[42,43]. ZnAF-2 is selectively bound to Zn^{2+}, but not bound to other divalent cations such as Ca^{2+}, Mg^{2+}, and Cu^{2+} [42]. Calcium Orange AM is a membrane-permeable Ca^{2+} indicator and was purchased from Molecular Probes, Inc. (Eugene, OR). The fluorescence indicators were dissolved in dimethyl sulfoxide and diluted to artificial cerebrospinal fluid (ACSF) containing 119 mM NaCl, 2.5 mM KCl, 1.3 mM $MgSO_4$, 1.0 mM NaH_2PO_4, 2.5 mM $CaCl_2$, 26.2 mM $NaHCO_3$, and 11 mM D-glucose (pH 7.3).

Hippocampal slice preparation. Rats were anesthetized with ether and decapitated under anesthesia. The brain was quickly removed from rats and bathed in ice-cold choline-ACSF, which consists of 124 mM choline chloride, 2.5 mM KCl, 2.5 mM $MgCl_2$, 1.25 mM NaH_2PO_4, 0.5 mM $CaCl_2$, 26 mM $NaHCO_3$, and 10 mM glucose (pH 7.3) to block excessive neuronal excitation. Horizontal hippocampal slices (400 μm) were prepared in

ice-cold choline-ACSF by using a vibratome ZERO-1 (Dosaka Kyoto, Japan). Hippocampal slices were placed in ACSF at 25 °C for at least 30 minutes. All solutions were continuously bubbled with 95% O_2 and 5% CO_2.

***In vitro* immunostaining.** Hippocampal slices were bathed in 50 μM $A\beta_{1-42}$ in ACSF for 15 min. Slices were then rinsed twice with ACSF for 5 min to remove extracellular agents, and fixed with paraformaldehyde (4% in 0.01 M PBS) for 15 min. Slices were rinsed in 0.01 M PBS three times. Slice tissues were blocked in 10% normal goat serum for 30 min, followed by rinse in 0.01 M PBS three times, incubated with 70% formic acid for 5 min, rinsed with 0.01 M PBS three times, and bathed at 4 °C in Aβ monoclonal antibody, 4G8 (COVANCE, 1:500 dilution in 0.01 M PBS) for 48 h. Slices were then rinsed with 0.01 M PBS three times, bathed in Alexa Fluor 633 goat anti-mouse IgG secondary antibody (1: 200 dilution in 0.01 M PBS) for 1 h, rinsed with 0.01 M PBS three times, bathed in 4′,6-diamidino-2-phenylindole (DAPI) for 10 min, rinsed again with 0.01 M PBS three times, and mounted on glass slides. Immunostaining images were obtained by using a confocal laser-scanning microscopic system (Nikon A1 confocal microscopes, Nikon Corp.) through a 10× objective. Florescence intensity was analyzed by the NIH Image J.

***Ex vivo* immunostaining.** Rats anesthetized with chloral hydrate (400 mg/kg) were placed in a stereotaxic apparatus. The skull was exposed and two burr holes were drilled. Injection cannulae (internal diameter, 0.15 mm; outer diameter, 0.35 mm) were bilaterally inserted into the dentate granule cell layer (4.0 mm posterior to the bregma, 2.3 mm lateral, 2.9 mm inferior to the dura) of the anesthetized rats. Thirty minutes later following recovery from the insertion damage, 50 μM $A\beta_{1-42}$ in ACSF, or 50 μM $A\beta_{1-42}$ with either 15 μM tetrodotoxin, a Na^{2+} channel blocker, 2 mM 6-cyano-7-nitroquinoxaline-2,3-dione (CNQX), an α-amino-3-hydroxy-5-methyl -4-isoxazolepropionate (AMPA) receptor antagonist, 500 μM chlorpromazine, a clathrin/caveolae-mediated endocytosis blocker, or 250 μM genistein, a caveolae/raft-mediated endocytosis blocker, in ACSF were bilaterally injected into the dentate granule cell layer at the rate of 0.25 μl/min for 8 min via the injection cannulae. Five minutes later, the brain was quickly removed from the rats and immunostaining images in hippocampal slices were obtained in the same manner except for changing the 10% goat serum with 5% goat serum. The positions of the injection cannulae were confirmed in the slice preparation.

***In vivo* intracellular Zn^{2+} imaging.** Fifty μM $A\beta_{1-42}$ in ACSF containing 100 μM ZnAF-2DA, or 50 μM $A\beta_{1-42}$ with either 15 μM tetrodotoxin, 2 mM CNQX, 500 μM chlorpromazine, or 250 μM genistein in ACSF containing 100 μM ZnAF-2DA was bilaterally injected via injection cannulae into the dentate granule cell layer of anesthetized rats at the rate of 0.25 μl/min for 8 min. Five minutes later, the hippocampal slices were prepared in the same manner. Slices were transferred to a chamber filled with ACSF, loaded with 2 μM Calcium Orange AM in ACSF for 30 min, and then rinsed in ACSF for 30 min. The hippocampal slices were transferred to a recording chamber filled with ACSF. The fluorescence of ZnAF-2 (laser, 488.4 nm; emission, 500–550 nm), and calcium orange (laser, 561.4 nm; emission, 570–620 nm) was measured with a confocal laser-scanning microscopic system (Nikon A1 confocal microscopes, Nikon Corp.). Calcium Orange AM was used to identify hippocampal regions in slices. The positions of the injection cannulae were confirmed in the slice preparation.

Data analysis. For multiple comparisons, differences between treated groups were analyzed by one-way ANOVA followed by post hoc testing using the Tukey's test. A value of $p < 0.05$ was considered significant (the statistical software, GraphPad Prism 5). Data were expressed as means ± standard error. The control group with vehicle was compared with the treated groups in all figures for the statistical analysis. In Fig. 1, Aβ group in the DG was also compared with those in the CA3 and the CA1.

Ethics statement. All experiments were done according to the Guidelines for the Care and Use of Laboratory Animals of the University of Shizuoka, which refer to American Association for Laboratory Animals Science and the guidelines laid down by the NIH (NIH Guide for the Care and Use of Laboratory Animals) in the USA. All experimental protocols were approved by the ethics committee of the University of Shizuoka

References

1. Nestor, P. J., Scheltens, P. & Hodges, J. R. Advances in the early detection of Alzheimer's disease. *Nat. Med.* **10**(Supp l), S34–S41 (2004).
2. Querfurth, H. W. & LaFerla, F. M. Alzheimer's disease. *N. Engl. J. Med.* **362**, 329–344 (2010).
3. Haass, C. *et al*. Amyloid beta-peptide is produced by cultured cells during normal metabolism. *Nature* **359**, 322–325 (1992).
4. Hardy, J. A. & Higgins, G. A. Alzheimer's disease: the amyloid cascade hypothesis. *Science* **256**, 184–185 (1992).
5. Gu, L., Tran, J., Jiang, L. & Guo, Z. A new structural model of Alzheimer's Aβ42 fibrils based on electron paramagnetic resonance data and Rosetta modeling. *J. Struct. Biol.* **194**, 61–67 (2016).
6. Schoonenboom, N. S. *et al*. Amyloid beta 38, 40, and 42 species in cerebrospinal fluid: more of the same? *Ann. Neurol.* **58**, 139–142 (2005).
7. Mucke, L. *et al*. High-level neuronal expression of abeta 1–42 in wild-type human amyloid protein precursor transgenic mice: synaptotoxicity without plaque formation. *J. Neurosci.* **20**, 4050–4058 (2000).
8. Masuda, Y. *et al*. Identification of physiological and toxic conformations in Abeta42 aggregates. *Chembiochem.* **10**, 287–295 (2009).
9. Xiao, Y. *et al*. Aβ(1–42) fibril structure illuminates self-recognition and replication of amyloid in Alzheimer's disease. *Nat. Struct. Mol. Biol.* **22**, 499–505 (2015).
10. Bush, A. I. The metal theory of Alzheimer's disease. *J. Alzheimers. Dis.* **33**(Suppl 1), S277–281 (2013).
11. Bush, A. I. *et al*. Rapid induction of Alzheimer A beta amyloid formation by zinc. *Science* **265**, 1464–1467 (1994).
12. Adlard, P. A. & Bush, A. I. Metals and Alzheimer's Disease: How Far Have We Come in the Clinic? *J. Alzheimers Dis.* **62**, 1369–1379 (2018).
13. Frederickson, C. J. *et al*. Concentrations of extracellular free zinc (pZn)e in the central nervous system during simple anesthetization, ischemia and reperfusion. *Exp. Neurol.* **198**, 285–293 (2006).
14. Takeda, A. *et al*. Amyloid β-mediated Zn^{2+} influx into dentate granule cells transiently induces a short-term cognitive deficit. *PLoS One* **9**, e115923 (2014).

15. Takeda, A. *et al*. Extracellular Zn^{2+} is essential for amyloid β_{1-42}-induced cognitive decline in the normal brain and its rescu. *J. Neurosci.* **37**, 7253–7262 (2017).
16. Takeda, A. *et al*. Novel defense by metallothionein induction against cognitive decline: from amyloid β_{1-42}-induced excess Zn^{2+} to functional Zn^{2+} deficiency. *Mol. Neurobiol.* **55**, 7775–7788 (2018).
17. Arispe, N., Rojas, E. & Pollard, H. B. Alzheimer disease amyloid ß protein forms calcium channels in bilayer membranes: Blockade by tromethamine and aluminum. *Proc. Natl. Acad. Sci. USA* **90**, 567–571 (1993).
18. Arispe, N., Rojas, E. & Pollard, H. B. Giant multilevel cation channels formed by Alzheimer disease amyloid ß protein [Aß-(1-40)] in bilayer membranes. *Proc. Natl. Acad. Sci. USA* **90**, 10573–10577 (1993).
19. Kawahara, M. Neurotoxicity of β-amyloid protein: oligomerization, channel formation and calcium dyshomeostasis. *Curr. Pharm. Des.* **16**, 2779–2789 (2010).
20. Arispe, N., Pollard, H. B. & Rojas, E. Zn^{2+} interactions with Alzheimer's amyloid ß protein calcium channels. *Proc. Natl. Acad. Sci. USA* **93**, 1710–1715 (1996).
21. Ullah, G., Demuro, A., Parker, I. & Pearson, J. E. Analyzing and Modeling the Kinetics of Amyloid Beta Pores Associated with Alzheimer's Disease Pathology. *PLoS One* **10**, e0137357 (2015).
22. Kwak, S. & Weiss, J. H. Calcium-permeable AMPA channels in neurodegenerative disease and ischemia. *Curr. Opin. Neurobiol.* **16**, 281–287 (2006).
23. Weiss, J. H. Ca permeable AMPA channels in diseases of the nervous system. *Front. Mol. Neurosci.* **4**, 42 (2011).
24. Yang, G. & Iadecola, C. Glutamate microinjections in cerebellar cortex reproduce cerebrovascular effects of parallel fiber stimulation. *Am, J, Physiol.* **271**, R1568–1575 (1996).
25. Suzuki, M., Fujise, Y., Tsuchiya, Y., Tamano, H. & Takeda, A. Excess influx of Zn^{2+} into dentate granule cells affects object recognition memory via attenuated LTP. *Neurochem. Int.* **87**, 60–65 (2015).
26. Takeda, A. *et al*. Maintained LTP and memory are lost by Zn^{2+} influx into dentate granule cells, but not Ca^{2+} influx. *Mol. Neurobiol.* **55**, 1498–1508 (2018).
27. Marchiando, A. M. *et al*. Caveolin-1-dependent occludin endocytosis is required for TNF-induced tight junction regulation *in vivo*. *J. Cell Biol.* **189**, 111–126 (2010).
28. Zhang, F., Guo, H., Zhang, J., Chen, Q. & Fang, Q. Identification of the caveolae/raft-mediated endocytosis as the primary entry pathway for aquareovirus. *Virology* **513**, 195–207 (2018).
29. Takeda, A. *et al*. Intracellular Zn^{2+} signaling in the dentate gyrus is required for object recognition memory. *Hippocampus* **24**, 1404–1412 (2014).
30. Minami, A. *et al*. Inhibition of presynaptic activity by zinc released from mossy fiber terminals during tetanic stimulation. *J. Neurosci. Res.* **83**, 167–176 (2006).
31. Freir, D. B., Holscher, C. & Herron, C. E. Blockade of long-term potentiation by beta-amyloid peptides in the CA1 region of the rat hippocampus *in vivo*. *J. Neurophysiol.* **85**, 708–713 (2001).
32. Whitcomb, D. J. *et al*. Intracellular oligomeric amyloid-beta rapidly regulates GluA1 subunit of AMPA receptor in the hippocampus. *Sci. Rep.* **5**, 10934 (2015).
33. Hyman, B. T., Van Hoesen, G. W., Damasio, A. R. & Barnes, C. L. Alzheimer's disease: cell-specific pathology isolates the hippocampal formation. *Science* **225**, 1168–1170 (1984).
34. Moryś., J., Sadowski, M., Barcikowska, M., Maciejewska, B. & Narkiewicz, O. The second layer neurones of the entorhinal cortex and the perforant path in physiological ageing and Alzheimer's disease. *Acta Neurobiol. Exp. (Wars)* **54**, 47–53 (1994).
35. Harris, J. A. *et al*. Transsynaptic progression of amyloid-β-induced neuronal dysfunction within the entorhinal-hippocampal network. *Neuron* **68**, 428–441 (2010).
36. Wesén, E., Jeffries, G. D. M., Dzebo, M. M. & Esbjörner, E. K. Endocytic uptake of monomeric amyloid-β peptides is clathrin- and dynamin-independent and results in selective accumulation of Aβ(1–42) compared to Aβ(1–40). *Sci. Rep.* **7**, 2021 (2017).
37. Ren, B. *et al*. Genistein: A Dual Inhibitor of Both Amyloid β and Human Islet Amylin Peptides. *ACS Chem. Neurosci.* **9**, 1215–1224 (2018).
38. LaFerla, F. M., Green, K. N. & Oddo, S. Intracellular amyloid-β in Alzheimer's disease. *Nat. Rev. Neurosci.* **8**, 499–509 (2007).
39. Shirwany, N. A., Payette, D., Xie, J. & Guo, Q. The amyloid beta ion channel hypothesis of Alzheimer's disease. *Neuropsychiatr. Dis. Treat.* **3**, 597–612 (2007).
40. Takeda, A., Koike, Y., Osawa, M. & Tamano, H. Characteristic of extracellular Zn^{2+} influx in the middle-aged dentate gyrus and its involvement in attenuation of LTP. *Mol. Neurobiol.* **55**, 2185–2195 (2018).
41. Takeda, A. & Tamano, H. Is vulnerability of the dentate gyrus to aging and amyloid-β_{1-42} neurotoxicity linked with modified extracellular Zn^{2+} dynamics? *Biol. Pharm. Bull.* **41**, 995–1000 (2018).
42. Hirano, T., Kikuchi, K., Urano, Y. & Nagano, T. Improvement and biological applications of fluorescent probes for zinc, ZnAFs. *J, Am, Chem, Soc.* **124**, 6555–6562 (2002).
43. Ueno, S. *et al*. Mossy fiber Zn^{2+} spillover modulates heterosynaptic *N*-methyl-*D*-aspartate receptor activity in hippocampal CA3 circuits. *J. Cell Biol.* **158**, 215–220 (2002).

Author Contributions

Planned experiments: H.T. and A.T. Performed the Experiments: N.O. and A.S. Analyzed data: P.A. and A.B. Wrote the paper: H.T. and A.T. All authors reviewed the manuscript.

Additional Information

Competing Interests: The authors declare no competing interests.

Publisher's note: Springer Nature remains neutral with regard to jurisdictional claims in published maps and institutional affiliations.